

## Visible light emission from GaAs nanocrystals in SiO<sub>2</sub> films fabricated by sequential ion implantation

Yoshihiko Kanemitsu,\* Hiroshi Tanaka, Yunosuke Fukunishi, and Takashi Kushida  
*Graduate School of Materials Science, Nara Institute of Science and Technology, Ikoma, Nara 630-0101, Japan*

Kyu Sung Min and Harry A. Atwater  
*Thomas J. Watson Laboratory of Applied Physics, California Institute of Technology, Pasadena, California 91125*

(Received 15 February 2000)

We have studied the mechanism of visible photoluminescence (PL) in GaAs nanocrystals in SiO<sub>2</sub> matrices formed by sequential ion implantation and thermal annealing. GaAs nanocrystal samples with the average diameter of  $\sim 6$  nm show a broad PL in the red spectral region. The PL peak energy of GaAs nanocrystals is blueshifted from that of the bulk GaAs crystal. Under resonant excitation at energies within the red PL band, the fine structures related to the LO phonon of the GaAs crystal are clearly observed in the PL spectrum at low temperatures. The excitation energy dependence of resonantly excited PL spectra shows that there are two different components of GaAs-related luminescence. In addition, in persistent luminescence hole-burning spectra, a pronounced hole is observed at the energy of the burning laser. The hole burnt in the luminescence spectrum has two structures related to the zero-phonon-line emission and the one-LO-phonon-assisted emission of delocalized excitons in GaAs nanocrystals. From resonantly excited PL spectra and luminescence hole-burning spectra, it is concluded that visible luminescence comes from both delocalized excitons and excitons bound to impurities in quantum-confined GaAs nanocrystals.

### I. INTRODUCTION

Semiconductor nanocrystals or quantum dots of sizes comparable to or smaller than the exciton Bohr radius in bulk materials are attracting much attention from the fundamental physics viewpoint.<sup>1</sup> Size-dependent optical and electrical properties of nanocrystals open a new field of materials physics and applications including light-emitting diodes, and single-electron transistors. Recent advances in controlling and characterizing semiconductor nanocrystals have generated considerable interest in exploring new synthesis techniques. A number of different techniques have been developed to synthesize semiconductor nanocrystals, including colloidal particles, gas-phase condensation, molecular beam epitaxy, and electrochemical etching.<sup>1,2</sup> One of the most versatile techniques for nanocrystal fabrication involves high-dose ion implantation.<sup>3,4</sup> In this method, almost any ions can be implanted into any solid substrate and thermal annealing leads to precipitation of nanocrystals from supersaturated solid solutions. The nanocrystal size and structure can be controlled by changing the ion dose, the kinetic energy of ions, and the annealing temperature.<sup>3,4</sup>

Very recently, it has been demonstrated that compound semiconductor nanocrystals in dielectric matrices are formed by sequential ion implantation.<sup>5,6</sup> For example, light-emitting GaAs nanocrystals are fabricated in amorphous matrices such as SiO<sub>2</sub> films.<sup>6</sup> For the study of GaAs nanocrystals or quantum dots, the embedded quantum structures have been usually used, e.g., GaAs in Al<sub>x</sub>Ga<sub>1-x</sub>As.<sup>2</sup> In these embedded structures, electronic properties of the Al<sub>x</sub>Ga<sub>1-x</sub>As barrier material strongly affect those of the GaAs/Al<sub>x</sub>Ga<sub>1-x</sub>As quantum systems. When the GaAs nanocrystal becomes small, the quantum-confinement effect pushes the  $\Gamma$ -like

conduction-band state of GaAs above the  $X$ -like conduction-band state of Al<sub>x</sub>Ga<sub>1-x</sub>As, leading to an indirect band system.<sup>7</sup> The high-barrier material is needed for the study of optical properties of the very small GaAs nanocrystal itself. SiO<sub>2</sub> has been used as a barrier material for a variety of semiconductor nanocrystals and has some advantages, because SiO<sub>2</sub> is a high confinement barrier for electrons and holes and has chemical and mechanical stability.<sup>1</sup> In addition, semiconductor nanocrystals embedded in SiO<sub>2</sub> matrices with low dielectric constants offer attractive options: (i) The total capacitance of nanocrystal systems decreases and the single-electron effects appear even at high temperatures. (ii) Nanocrystal/SiO<sub>2</sub> structures have a potential for applications to optical waveguides and photonic devices.

In this paper, we have studied photoluminescence (PL) properties of GaAs nanocrystals formed by Ga<sup>+</sup> and As<sup>+</sup> implantation into SiO<sub>2</sub> films followed by thermal annealing. In the sample annealed at 900 °C for 60 min, GaAs nanocrystals with  $\sim 6$  nm diameter are formed in SiO<sub>2</sub> films. A broad PL due to GaAs nanocrystals is observed in the red spectral region. From pico- and nanosecond PL dynamics, resonantly excited PL, and luminescence hole-burning experiments, it is concluded that the red PL band is due to free-exciton and bound-exciton emission in GaAs nanocrystals. The luminescence mechanism of GaAs nanocrystals will be discussed.

### II. EXPERIMENT

Sequential ion implantation followed by thermal annealing was used to form GaAs nanocrystals in SiO<sub>2</sub> films. As ion implantation often introduces structural damage into SiO<sub>2</sub> matrices, thermal annealing is very important for the formation of GaAs nanocrystals and the reduction of defects

as nonradiative recombination centers. In this work, we tried to fabricate GaAs nanocrystals showing visible light emission by changing annealing temperature and annealing time.

Ga<sup>+</sup> ions were first implanted and then As<sup>+</sup> ions were implanted at 75 keV into the 100-nm SiO<sub>2</sub> on (100) crystalline Si substrates. The doses of Ga and As ions were  $3 \times 10^{16}$  and  $2 \times 10^{16} \text{ cm}^{-2}$ , respectively. The peaks of implanted Ga and As ions match both spatially and in concentration. Subsequent annealing in vacuum resulted in precipitation of GaAs nanocrystals. We have performed isochronal and isothermal annealing experiments in order to enhance PL intensity from samples. For a fixed annealing time of 10 min, the annealing temperature was varied between 800 and 1100 °C. For a fixed annealing temperature of 900 °C, the annealing time was varied between 0 and 300 min.

For visible and near-infrared PL measurements, a 488-nm Ar-ion laser was used as an excitation source and the PL signals were dispersed by a 27-cm monochromator and detected by a Ge diode detector or a cooled charge-coupled detector (CCD) camera. For resonantly excited PL and visible PL measurements, a wavelength-tunable Ti:Al<sub>2</sub>O<sub>3</sub> and a dye-laser system were used, and the PL spectra were measured by a 50-cm double-grating monochromator and detected by a photomultiplier. Time-resolved PL spectra were measured using a streak camera. The spectral sensitivity of the measuring system was calibrated using a tungsten standard lamp. The samples were mounted on the cold finger of a temperature-variable closed-cycle He gas cryostat during the measurements.

### III. RESULTS AND DISCUSSION

#### A. Thermal annealing and photoluminescence spectrum

In order to clarify the correlation between PL spectra and annealing conditions, we studied PL spectra of annealed samples in the visible and near-infrared spectral region. As-implanted samples show a very weak and broad PL band near 2.3 eV.<sup>8</sup> In as-implanted samples, no GaAs nanocrystals exist. Similar PL has been observed even in Si<sup>+</sup>- or Ge<sup>+</sup>-implanted SiO<sub>2</sub> samples.<sup>9</sup> The ~2.3-eV PL is due to the radiative defect centers in the SiO<sub>2</sub> film. However, after thermal annealing at high temperatures, the ~2.3-eV PL band disappears and a new PL band appears in the red spectral region. The red PL intensity depends on the thermal annealing condition.

Figure 1 shows PL spectra of samples as a function of the annealing temperature for a fixed annealing time of 10 min. The PL spectra were measured by a cooled Ge detector under 2.540-eV laser excitation at 14 K. For the unannealed (as-prepared) samples, the PL band is not observed in the red and infrared spectral region. The red PL is clearly observed in samples annealed at 900 and 1000 °C. For lower or higher annealing temperatures, the red PL band does not appear. In addition to the red PL band, the samples show some PL bands in the near-infrared (1–1.4- $\mu\text{m}$ ) spectral region. From the temperature dependence of the PL intensity,<sup>8</sup> it has been concluded that the near-infrared PL bands in the 1–1.4- $\mu\text{m}$  region are due to radiation damage centers in the Si substrate<sup>10,11</sup> and the Ga-vacancy–Si complexes in GaAs nanocrystals.<sup>12</sup>

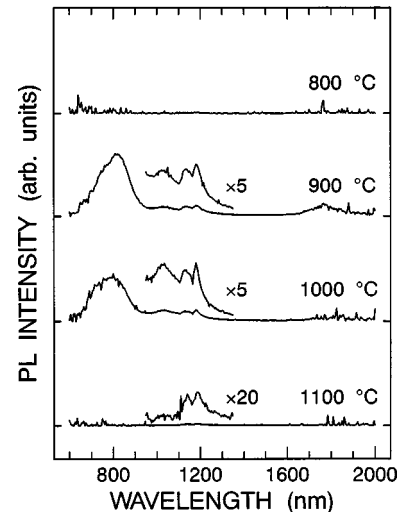


FIG. 1. PL spectra of samples in the red and near-infrared spectral region under 488-nm laser excitation at 14 K as a function of the annealing temperature for a fixed annealing time of 10 min.

Figure 2 shows PL spectra of samples as a function of the annealing time for a fixed annealing temperature of 900 °C. For samples annealed longer than 120 min, the red PL is not observed. At lower annealing temperatures or shorter annealing times, GaAs nanocrystals are not formed in the sample. At higher annealing temperatures or longer annealing times, it is speculated that the evaporation of As occurs as discussed in Ref. 13. Therefore, red luminescence is observed in the samples annealed at 900 °C for 10–60 min. The PL intensity of Ga<sup>+</sup>- and As<sup>+</sup>-implanted samples (compound semiconductor samples) is sensitive to the annealing condition, compared to the case of Si<sup>+</sup>- or Ge<sup>+</sup>-implanted samples (elemental semiconductor samples).<sup>9</sup>

In the samples showing red PL, the presence of nanocrystalline GaAs was verified from lattice images of high-resolution electron transmission micrographs (TEM). As an example, Fig. 3(a) shows the TEM image of the sample annealed at 900 °C for 60 min. After thermal annealing, GaAs nanocrystals appear in the sample. The size distribution of

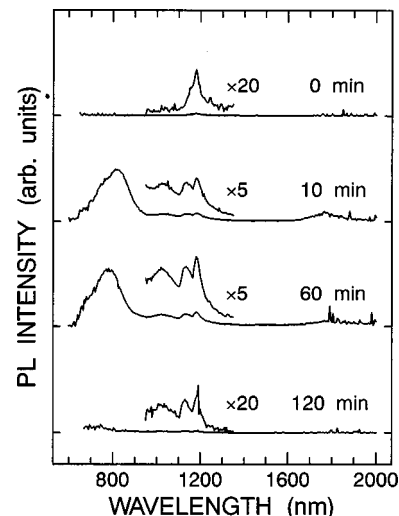


FIG. 2. PL spectra of samples in the red and near-infrared spectral region under 488-nm laser excitation at 14 K as a function of the annealing time at a fixed annealing temperature of 900 °C.

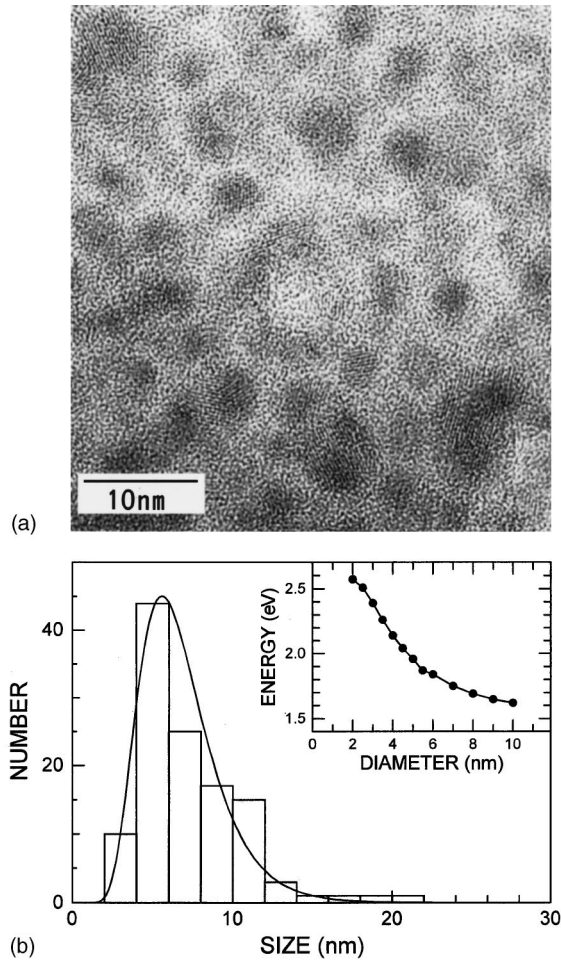


FIG. 3. (a) Transmission electron micrograph (TEM) image of the sample annealed at 900 °C for 60 min. (b) The size distribution of GaAs nanocrystals determined from the TEM image. The inset shows the theoretical calculation of the size dependence of the exciton energy in GaAs nanocrystals (the data are reproduced from Ref. 15).

GaAs nanocrystals determined from TEM observations is shown in Fig. 3(b). The size distribution is approximately described by a log-normal function,<sup>14</sup> as shown by the solid line in Fig. 3(b). The average size of GaAs nanocrystals is estimated to be about 6.3 nm. There is a good correlation between the red PL band and the presence of GaAs nanocrystals. Hereafter, we will discuss the luminescence properties of GaAs nanocrystals in SiO<sub>2</sub> matrices and the mechanism of the red PL by using the sample annealed at 900 °C for 60 min.

Figure 4 shows, in more detail, a global PL spectrum of the sample annealed at 900 °C for 60 min in the visible and near-infrared spectral region at 7 K. The PL spectrum was measured by a cooled Ge detector and a cooled CCD camera under 2.540-eV laser excitation. The peak energy of the PL band (~1.6 eV) is above the exciton energy of bulk GaAs crystal at 7 K (~1.515 eV). Therefore, one is led to believe that the quantum-confinement states of GaAs nanocrystals are one of the origins of red PL. However, the broad luminescence band of GaAs nanocrystals can be divided into two Gaussian bands (broken lines in Fig. 4): the high-energy *F* band and the low-energy *B* band. The red luminescence may share different origins.

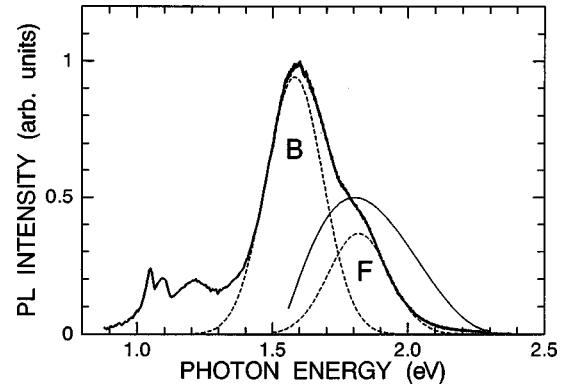


FIG. 4. PL spectra of GaAs nanocrystals in SiO<sub>2</sub> matrices under 2.540 eV at 7 K. The full PL spectrum can be divided into two Gaussian bands (broken curves). The free-exciton emission spectrum of GaAs nanocrystals (the thin solid curve) is calculated from the size distribution and the size dependence of the exciton energy in Fig. 3(b).

As shown in Fig. 3(b), the size distribution of GaAs nanocrystals can be described by the log-normal function. Using the solid line in Fig. 3(b), we can estimate the free-exciton emission spectrum of the sample. Here, we assume the PL efficiency does not depend on the nanocrystal size and we use the theoretically calculated results in Ref. 15 as the relationship between the nanocrystals size and the exciton energy. The size dependence of the exciton energy in GaAs nanocrystals is illustrated in the inset of Fig. 3(b) (the data are reproduced from Ref. 15). The calculated exciton energy spectrum for our sample is shown by a thin solid curve in Fig. 4. The spectral shape of the *F* band is consistent with that of the calculated exciton energy spectrum. Therefore, it is believed that the *F* band is due to the delocalized-exciton (free-exciton) emission in quantum-confined GaAs nanocrystals whose band-gap energy is blueshifted from that of bulk GaAs crystal. However, the low-energy *B* band cannot be explained by the free-exciton emission from GaAs nanocrystals. In the following sections, we study the origin of the *F* and *B* bands by means of time-resolved PL spectra measurements and resonant excitation spectroscopy.

## B. Photoluminescence decay dynamics

In the previous section, we showed that there is a good correlation between the appearance of the red PL band and the presence of GaAs nanocrystals and that the red PL band in the sample annealed at 900 °C for 60 min can be divided into two Gaussian bands (the *F* and *B* bands). In order to discuss the origin of the *F* and *B* bands, we have studied PL decay dynamics in the pico- and nanosecond time region at low temperatures.

Figure 5 shows PL decay profiles at different emission energies [(a) 1.878, (b) 1.721, (c) 1.653, and (d) 1.549 eV] under 3.10-eV and 1.1-ps laser excitation at 10 K. The PL decay curves show nonexponential and they are approximately fitted by three exponential components (solid curves in the figure). Since the decay profiles,  $I(t)$ , have essentially the same nonexponential shape at different emission energies, the mean PL lifetime,  $\tau_{PL}$ , is defined by<sup>16</sup>

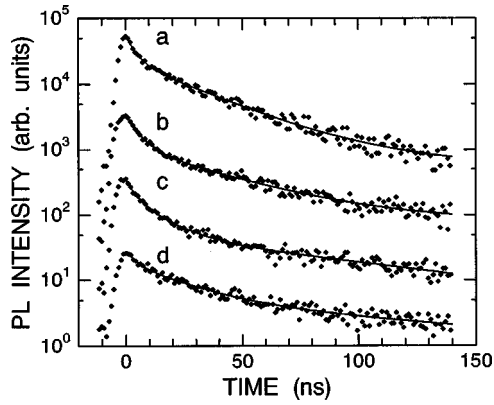


FIG. 5. PL decay dynamics in GaAs nanocrystals in  $\text{SiO}_2$  matrices at 10 K for different phonon energies: (a) 1.878, (b) 1.721, (c) 1.653, and (d) 1.549 eV. The PL decay profiles were measured under 3.10-eV, 1.1-ps laser excitation.

$$\tau_{\text{PL}} = \frac{1}{I_0} \int I(t) dt,$$

where  $I_0$  is the initial PL intensity just after pulsed laser excitation.

The mean lifetimes,  $\tau_{\text{PL}}$ , are very sensitive to the emission photon energy, and they are summarized as a function of phonon energy in Fig. 6. The lifetime is  $\sim 20$  ns in the *F* band, while the lifetime is longer than  $\sim 50$  ns in the *B* band. The PL dynamics experiments show that the origin of the *F* band is different from that of the *B* band. In addition, these PL lifetimes in GaAs nanocrystals are longer than those of the free-exciton emission in bulk GaAs crystal, one-dimensional (1D) GaAs wires,<sup>17</sup> and 2D GaAs wells.<sup>18</sup> The slow and nonexponential PL decay curves have been usually observed in other nanocrystal systems such as CuCl (Ref. 19) and CdSe (Refs. 20 and 21).

In small nanocrystals, the exciton exchange energy increases with a decrease of the nanocrystal size.<sup>22</sup> The lowest excitonic state is split due to the exchange interaction between holes and electrons. The lower level is the optically forbidden state and the upper level is the optically allowed state. This exciton exchange splitting is one of the candidates

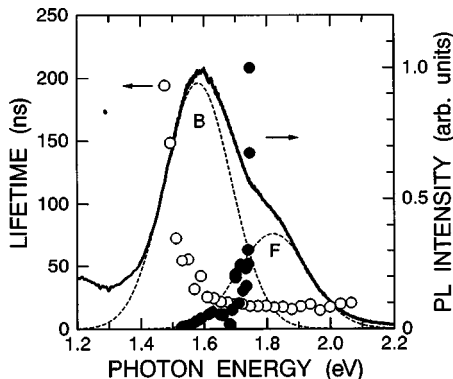


FIG. 6. PL lifetime ( $\circ$ ) and the LO-phonon related PL intensity ( $\bullet$ ) as a function of the photon energy. The PL lifetime was measured under 3.10-eV, 1.1-ps laser excitation at 10 K. The PL lifetime in the *B* band is longer than that in the *F* band. The PL intensity increases under resonant excitation at energies within the *F* band.

for the origin of the long lifetime and nonexponential PL decay in nanocrystals.<sup>21</sup> However, the exciton exchange splitting of GaAs nanocrystals is small, compared to the case of CdSe nanocrystals.<sup>22</sup> In particular, in our 6-nm GaAs nanocrystals, the exciton exchange splitting is estimated to be negligibly small. This consideration is supported by the luminescence hole-burning experiment as will be shown in the Sec. III D. Therefore, it is believed that the long PL lifetime and the nonexponential PL dynamics in GaAs nanocrystals are caused by the shallow-trap and/or impurity states, rather than the formation of optically forbidden excitonic states in nanocrystals.<sup>21,23</sup> The long PL lifetime and the lower-energy PL below the band-gap energy of GaAs nanocrystals suggest that the *B* band is due to localized excitons in shallow-trap and impurity states in GaAs nanocrystals.

### C. Resonantly excited luminescence

Under blue or green laser excitation (nonresonant excitation), the samples show broad luminescence even at low temperatures, as shown in Fig. 4. The global PL spectrum (or nonresonantly excited PL spectrum) contains contributions from all nanocrystals and other luminescent centers. The broad PL spectrum is due to the sample inhomogeneities such as the size distribution and impurities in nanocrystals. These sample inhomogeneities are the origin of nonexponential PL decay. As in many inhomogeneously broadened systems, resonant excitation results in fluorescence line narrowing (FLN) in nanocrystal samples.<sup>21,23,24</sup> The resonantly excited PL spectra (FLN spectra) are sensitive to the nature of the band-edge structure and the trap state.<sup>23,24</sup> Resonant excitation spectroscopy is one of powerful methods used to obtain intrinsic information from inhomogeneously broadened spectra.

Under resonant excitation at energies within the PL band, we can observe fine structures in PL spectra at low temperatures. Figure 7 shows resonantly excited PL spectra at 7 K of the sample annealed at 900 °C for 60 min. The excitation laser energies are shown in the figure. A sharp PL peak marked by a solid circle appears in the resonantly excited PL spectra. The energy difference between the sharp peak and the excitation laser is  $\sim 36$ – $37$  meV. The observed energy difference agrees well with the LO-phonon energy of bulk GaAs crystal (36.5 meV).<sup>25</sup> In addition to this sharp peak, broad PL spectra with multiplex structures are observed at the lower-energy side of excitation laser energies; as an example, the PL spectrum under 1.745-eV excitation. Here, we define the luminescence Stokes shift as the energy difference between the PL peak and the excitation laser.

The luminescence Stokes shifts are summarized, as a function of the excitation laser energy, in Fig. 8. There are two different components: One is the excitation-energy-independent PL peak ( $\bullet$  in Fig. 8) and the others are the excitation-energy-dependent PL peaks with large Stokes shift ( $\circ$ ,  $\triangle$ , and  $\square$  in Fig. 8). The energy intervals between the peaks (solid lines in Fig. 8) are almost equal to the GaAs LO-phonon energy.<sup>26</sup> The lower-energy peaks ( $\triangle$  and  $\square$ ) are LO-phonon replicas of the high-energy peak ( $\circ$ ). These resonantly excited PL spectra show that two different origins are related to GaAs nanocrystals.

The LO-phonon-assisted PL intensity depends strongly on the excitation photon energy. The PL intensity at the sharp

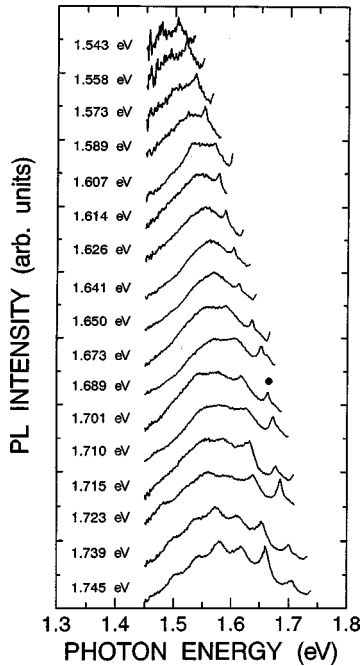


FIG. 7. PL spectra of GaAs nanocrystals in  $\text{SiO}_2$  matrices under various excitation energies at 7 K. The excitation laser energies are shown in the figure. Fine structures related to the LO phonon of GaAs nanocrystals are observed under resonant excitation at energies within the  $F$  band.

peak (● in Figs. 7 and 8) is plotted as a function of the excitation energy in Fig. 6. The LO-phonon-related peak appears when the excitation laser energy is higher than the band-gap energy of the bulk GaAs ( $\sim 1.51$  eV). The GaAs LO-phonon-assisted PL intensity increases dramatically when the excitation energy is within the  $F$  band. This PL excitation spectrum shows that the sharp PL peak comes from the photoabsorption state under resonant excitation. The excitation-energy-independent PL peak (● in Fig. 8) is due to the one-LO-phonon-assisted luminescence of free excitons.

Resonantly excited PL spectra (FLN spectra) show that there are two different components of GaAs-related luminescence. It is concluded that the  $F$  band is due to the delocalized-exciton (free-exciton) emission in GaAs nano-

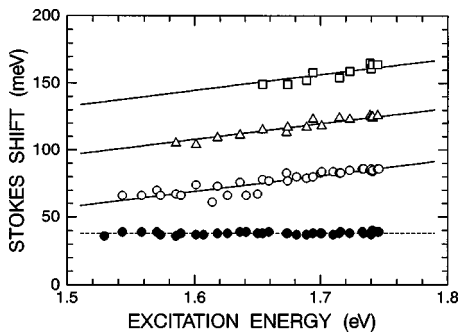


FIG. 8. Luminescence Stokes shifts as a function of the excitation energy. There are two different components of luminescence: One is the excitation-energy-independent PL band (●) and the other is the excitation-energy-dependent PL band with a large Stokes shift (○, △, and □). The energy intervals between solid lines are equal to the LO-phonon energy of the GaAs crystal.

crystals and the  $B$  band with GaAs LO-phonon replicas is due to localized-exciton emission in shallow-trap states in GaAs nanocrystals.

#### D. Phonon-assisted luminescence and luminescence hole burning

In the previous section, it is shown that LO-phonon-assisted luminescence is clearly observed in GaAs nanocrystals under resonant excitation at low temperatures. In this section, let us discuss the origin of phonon-assisted luminescence in GaAs nanocrystals.

It has been theoretically predicted that a small GaAs nanocrystal becomes an indirect-gap semiconductor and the lowest optical transition is the  $\Gamma$ - $X$  transition.<sup>27</sup> The indirect  $\Gamma$ - $X$  transition energy is 1.9 eV in bulk GaAs crystal.<sup>25</sup> It is estimated that the  $\Gamma$ - $X$  transition is the lowest transition in very small nanocrystals whose band gap is above  $\sim 2.3$  eV.<sup>15,27</sup> If the phonon-assisted PL is caused by the momentum-conserving phonon-assisted  $\Gamma$ - $X$  transition, one should observe the phonon structures in the higher-energy region near  $\sim 2.3$  eV. However, the phonon replicas are observed in the 1.6–1.7-eV region, shown in Fig. 7. The observed energy region is much lower than the indirect  $\Gamma$ - $X$  transition energy in bulk GaAs crystal<sup>25</sup> and the theoretically predicted energy region.<sup>15,27</sup> Therefore, it is believed that the observed phonon-assisted PL is not due to the phonon-assisted transition in indirect-gap GaAs nanocrystals.

Moreover, we have studied luminescence hole-burning (LHB) spectra<sup>28</sup> in order to discuss the zero-phonon-line emission and phonon-assisted emission of excitons and to determine whether the GaAs nanocrystal is a direct- or an indirect-gap semiconductor. In the LHB experiments, the sample is excited by intense laser at the energy within the PL band. After prolonged laser irradiation (burning laser excitation), a spectral hole is formed near the burning laser energy in the luminescence band. The LHB affords us similar information as does the FLN. However, in the resonantly excited PL or FLN spectra, it is difficult to obtain the detailed spectrum near the excitation energy because of the scattering of the excitation laser light. In the LHB experiment, it is comparatively easy to observe the spectral change just at the excitation energy.

Figure 9 shows global PL spectra of the sample before and after the burning laser irradiation at 10 K. The luminescence spectra were measured by a cooled charge-coupled device (CCD) camera under 2.540-eV laser excitation. The dotted line shows the PL spectrum before the burning laser irradiation. The samples were kept at 10 K and were exposed to the burning laser of  $\sim 6.5$  W/cm<sup>2</sup> at 1.713 eV for 20 min. The solid line shows the PL spectrum after the burning laser irradiation. The inset shows, in more detail, the PL spectral change near the burning laser energy. A pronounced spectral change is observed near the burning laser energy. The spectral holes in the PL spectrum recovered after thermal annealing at high temperatures above 100 K.<sup>29</sup> From reversible hole-burning phenomena, it is believed that the photoionization of nanocrystals leads to the persistent LHB phenomena.<sup>29,30</sup>

The PL intensity changes,  $(I_a - I_b)/I_b$ , are summarized in Fig. 10, where  $I_b$  and  $I_a$  are the PL intensities before and after the burning laser irradiation ( $\sim 6.5$  W/cm<sup>2</sup> for 10 min)

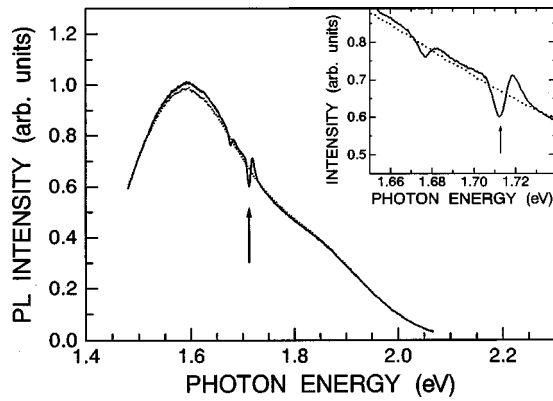


FIG. 9. Global photoluminescence spectra of GaAs nanocrystals before (dotted line) and after the burning laser irradiation (1.713 eV and 6.5 W/cm<sup>2</sup>) for 20 min at 10 K (solid line). The inset shows luminescence spectra near the burning laser energy. The PL spectra were measured under 2.540-eV laser excitation.

at 10 K, respectively. In persistent LHB spectra, the spectral hole is clearly observed at the burning laser energies of (a) 1.737, (b) 1.663, and (c) 1.553 eV. The largest hole is observed at the burning energy, as shown in Fig. 10. This behavior is similar to the case of other direct-gap semiconductors,<sup>30</sup> but different from the case of indirect-gap semiconductor Si.<sup>31</sup> Our GaAs nanocrystal sample behaves as a direct-gap semiconductor. Moreover, the peak energy at the hole coincides with the energy of the burning laser within the experimental resolution ( $<0.5$  meV). There is no energy gap between the photoabsorption and the light-emission states; The exciton exchange splitting is not clearly observed in GaAs nanocrystals under our experimental conditions.

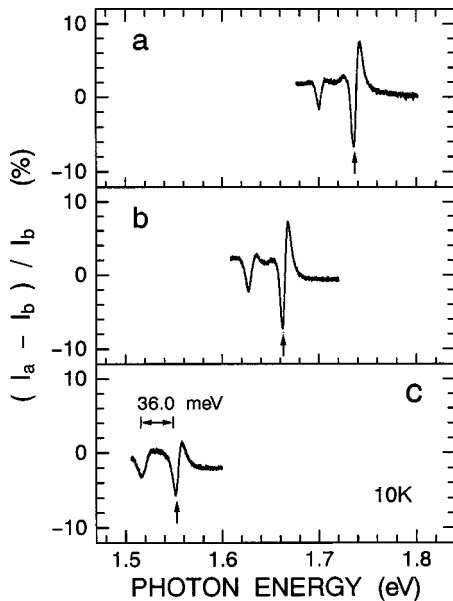


FIG. 10. Persistent luminescence-hole-burning spectrum,  $(I_a - I_b)/I_b$ , of GaAs nanocrystals at 10 K.  $I_a$  and  $I_b$  are the luminescence intensities after and before the burning laser irradiation ( $\sim 6.5$  W/cm<sup>2</sup> for 10 min), respectively. The PL spectra were measured under 2.540-eV laser excitation. The burning laser energies are shown by the arrows: (a) 1.737, (b) 1.663, and (c) 1.553 eV. The energy difference between the main and side holes is 36.0 meV, which corresponds to the LO-phonon energy of the GaAs crystal.

The GaAs nanocrystal sample shows the zero-phonon-line emission with no Stokes shift.

In addition, Fig. 10 shows that the other spectral hole is observed at the lower-energy region below the burning laser energy. The energy difference between the burning laser and the lower-energy hole is 36.0 meV, which is equal to the LO-phonon energy of GaAs crystal. The spectral hole at the low-energy region in the LHB spectra corresponds to the one-LO-phonon-assisted emission in the resonantly excited PL spectra (sharp peak marked by ● in Fig. 7). Because of the quantum confinement of excitons,<sup>32,33</sup> the coupling of free excitons with phonons is enhanced in small dimensions, compared to the case of the bulk GaAs crystal. Phonon-assisted optical transitions are also important in the luminescence process in a direct-gap GaAs nanocrystal semiconductor.

In our GaAs nanocrystals, however, we cannot observe holes at the 2LO-phonon energy position below the zero-phonon line in LHB spectra. If the LO-phonon-assisted optical transitions dominate the light-absorption and light-emission processes, holes will appear at the 2LO-phonon energy position below the excitation laser energy (one-LO-phonon emission during both light absorption and light emission). However, the observation of no pronounced hole at the 2LO-phonon energy shows that the probability of the phonon-assisted light-absorption process is negligibly small, compared to the direct light-absorption (zero-phonon light-absorption) process. This observation is different from PL spectra of direct-gap II-VI compound nanocrystals; for example, in CdSe nanocrystals, a 2LO-phonon replica of the delocalized-exciton emission is clearly observed.<sup>34,35</sup> This difference suggests that the strength of the coupling between excitons and LO phonons in GaAs nanocrystals is weaker than that in CdSe nanocrystals. In addition, in CdSe nanocrystals, the lowest excited state is the optically forbidden one, because of the exciton exchange interaction, as discussed above. From the FLN and LHB spectra, it is concluded that the exciton exchange splitting is negligibly small and the coupling strength between the lowest excitons and phonons in GaAs nanocrystals is weaker than that in II-VI (Refs. 34–37) and I-VII nanocrystals.<sup>32,33</sup> However, the size dependence of the exciton-phonon couplings in semiconductor nanocrystals is not clear,<sup>36,37</sup> and the mechanism is under discussion.<sup>34–39</sup> Further experimental studies in different materials and structures (free-standing or rigid-boundary conditions) are needed for the understanding of the nature of the exciton-phonon couplings in nanocrystals.

In the LHB spectrum, two holes are only observed at energies of the zero-phonon emission and the one-LO-phonon-assisted emission of free excitons. The other holes are not observed in the lower-energy region (see, as an example, Fig. 9). The lower-energy LO-phonon replicas are observed in resonantly excited PL spectra (○, △, and □ in Fig. 8), but not in the LHB spectra. The difference between PL and LHB spectra suggests that the LO-phonon-assisted PL in the lower-energy region is not due to the free-exciton emission in GaAs nanocrystals. When excitons are bound to the shallow impurity centers, the exciton-phonon coupling becomes strong. The LO-phonon replica is clearly observed in impurity-related PL spectra even in bulk GaAs crystal.<sup>12</sup> In addition, since the density of states of shallow impurity

states is small, it is considered that the impurity state does not cause pronounced holes in the LHB spectra. From the difference between PL and LHB spectra, it is concluded that the lower-energy PL ( $\circ$  in Fig. 8) is caused by excitons bound to impurities in GaAs nanocrystals.

The LHB experiments clearly show that our GaAs nanocrystals are direct-gap band structures and the phonon-assisted PL is not due to the momentum-conserving phonon-assisted  $\Gamma$ - $X$  transition in indirect-gap GaAs nanocrystals. By comparison between the PL and LHB spectra, the phonon-related peak marked by  $\bullet$  in Fig. 7 is due to the one-LO-phonon-assisted emission of free excitons. There is a good correlation between the resonantly excited PL and the LHB spectra.<sup>40</sup> The zero-phonon-line emission and one-LO-phonon-assisted emission of free excitons clearly appear in both the resonantly excited PL and the LHB spectra. On the other hand, the LO-phonon structures with a large Stokes shift ( $\circ$  in Fig. 8) can be explained by a picture that excitons are localized at the lower-energy impurity states.

#### E. Bound-exciton emission

The resonant excitation spectroscopy (FLN and LHB spectra) shows that there are two different PL bands related to GaAs nanocrystals and that both delocalized (“free”) excitons and excitons bound to impurities in GaAs nanocrystals contribute to visible PL. In Si and GaAs semiconductors, the PL intensity due to excitons bound to impurities are very sensitive to the hydrogen concentration in the sample.<sup>41–43</sup> The hydrogen (or deuterium) effect on luminescence in GaAs nanocrystal samples has been studied.<sup>44</sup> After high-dose deuterium implantation ( $6 \times 10^{15} \text{ cm}^{-2}$ ), the lower-energy  $B$  band disappears.<sup>44</sup> It is known that in Si and GaAs semiconductors hydrogenation (the hydrogen or deuterium introduction) causes the neutralization of dopants and defects and a reduction of the PL intensity due to excitons bound to donors and acceptors.<sup>41–43</sup> Therefore, the deuterium implantation experiments support that the lower-energy PL band (the  $B$  band) is due to impurity-bound excitons in GaAs nanocrystals. Since our samples are fabricated by precipitation of GaAs nanocrystals from supersaturated solid solutions (Ga and As in  $\text{SiO}_2$ ), GaAs nanocrystals may contain Si impurities acting as donors or acceptors.

When excitons are bound to the shallow or deep impurity centers, the exciton-phonon coupling becomes strong. Even in the direct-gap semiconductor bulk GaAs crystal, the LO-phonon replica is clearly observed in impurity-related PL spectra.<sup>12</sup> The shallow Si impurity states produce a sharp luminescence with LO-phonon replicas even in the bulk GaAs crystal.<sup>12</sup> The radius of the first Bohr orbit of the Si acceptor impurity is calculated by a hydrogenic model and is about 1.6 nm. In very small nanocrystals, the impurity state may show size-dependent optical responses.<sup>45</sup> Therefore, it is considered that the size-dependent bound-exciton emission causes the excitation-energy dependence of the LO-phonon-assisted emission at the lower-energy region, as shown in Fig. 8. Excitons bound to impurities in quantum-confined GaAs nanocrystals cause the  $B$  band with LO-phonon replicas. The  $F$  and  $B$  bands are due to the delocalized and bound excitons in GaAs nanocrystals, respectively. Because of quantum confinement of excitons, the coupling of free and bound excitons with phonons is enhanced. Phonon-assisted

radiative transitions of free and bound excitons are clearly observed in GaAs nanocrystals.

We observed the delocalized-exciton and bound-exciton emission of quantum-confined GaAs nanocrystals in  $\text{SiO}_2$  matrices fabricated by ion-implantation and thermal annealing techniques. The exciton-related PL in GaAs nanocrystals prepared by colloidal methods has not been reported because of insufficient surface passivation.<sup>46,47</sup> Therefore, it is concluded that sequential ion implantation followed by thermal annealing can be used to produce semiconductor nanocrystals with low defect density. The synthesis of compounds by implantation of the individual constituents is a simple method to produce light-emitting compound semiconductor nanostructures.

#### IV. CONCLUSIONS

In conclusion, we have fabricated light-emitting GaAs nanocrystals by sequential ion implantation of Ga and As followed by thermal annealing and have discussed the origin of visible light emission from GaAs nanocrystals in  $\text{SiO}_2$  matrices. There is a good correlation between the appearance of the red PL band and the presence of GaAs nanocrystals in the samples. The red PL band in the sample annealed at 900 °C for 60 min can be divided into two Gaussian bands: the higher-energy  $F$  and the lower-energy  $B$  bands. Under resonant excitation at energies within the red PL band, fine structures related to the GaAs LO phonon are clearly observed. The PL intensity increases dramatically when the excitation energy is within the  $F$  band. There are two different components of the LO-phonon-assisted luminescence: One is the one LO-phonon-assisted emission of free excitons and the others are the LO-assisted emission of bound excitons. Phonon-assisted optical transitions are important in the luminescence process, because of the quantum confinement of excitons in small dimensions. In addition, in persistent luminescence hole-burning spectra, a pronounced hole is observed at the energy of the burning laser. The spectral hole burnt in the luminescence spectrum has two structures related to the zero-phonon-line emission and the one-LO-phonon-assisted emission of free excitons in GaAs nanocrystals. From resonantly excited PL spectra and luminescence hole-burning spectra, it is concluded that the higher-energy  $F$  band is due to the free-exciton emission and the lower-energy  $B$  band is due to the bound-exciton emission. Visible luminescence comes from both delocalized excitons and excitons bound to impurities in quantum-confined GaAs nanocrystals.

#### ACKNOWLEDGMENTS

The authors would like to thank Dr. S. Okamoto and S. Mimura for discussions. This work was partly supported by a Grant-In-Aid for Scientific Research (B) from the Japan Society for the Promotion of Science (No. 11440095), The Corning Research Grand Award, and The Yazaki Foundation for Science and Technology.

- \* Author to whom correspondence should be addressed. Electronic address: sunyu@ms.aist-nara.ac.jp
- <sup>1</sup> See, for example, J. Lumin. **70**, (1–6) (1996), special issue on spectroscopy of isolated and assembled semiconductor nanocrystals, edited by L. E. Brus, Al. L. Efros, and T. Itoh.
- <sup>2</sup> See, for example, A. Zunger, Mater. Res. Bull. **23**, 15 (1998).
- <sup>3</sup> See, for example, C. W. White, J. D. Budai, S. P. Withrow, J. G. Zhu, E. Sonder, R. A. Zuhr, A. Meldrum, D. M. Hembree, Jr., D. O. Henderson, and S. Praver, Nucl. Instrum. Methods Phys. Res. B **141**, 228 (1998).
- <sup>4</sup> See, for example, H. A. Atwater, K. V. Shcheglov, S. S. Wong, K. J. Vahala, R. C. Flagan, L. Brongersma, and A. Polman, in *Materials Synthesis and Processing Using Ion Beams*, edited by R. J. Culbertson, K. S. Jones, O. W. Holland, and K. Maex, MRS Symposia Proceedings No. 316 (Materials Research Society, Pittsburgh, 1994), p. 409.
- <sup>5</sup> C. W. White, J. D. Budai, J. G. Zhu, S. P. Withrow, R. A. Zuhr, D. M. Hembree, Jr., D. O. Henderson, A. Ueda, Y. S. Tung, R. Mu, and R. H. Magruder, J. Appl. Phys. **79**, 1876 (1996).
- <sup>6</sup> S. Okamoto, Y. Kanemitsu, K. S. Min, and H. A. Atwater, Appl. Phys. Lett. **78**, 1829 (1998).
- <sup>7</sup> A. Franceschetti and A. Zunger, Phys. Rev. B **52**, 14 664 (1995).
- <sup>8</sup> Y. Kanemitsu, H. Tanaka, T. Kushida, K. S. Min, and H. A. Atwater, J. Appl. Phys. **86**, 1762 (1999).
- <sup>9</sup> Y. Kanemitsu, N. Shimizu, S. Okamoto, T. Komoda, P. L. F. Hemment, and B. J. Sealy, in *Advances in Microcrystalline and Nanocrystalline Semiconductors—1996*, edited by R. W. Collins, P. M. Fauchet, I. Shimizu, J. C. Vial, T. Shimada, and A. P. Alivisatos, MRS Symposia Proceedings No. 456 (Materials Research Society, Pittsburgh, 1997), p. 99.
- <sup>10</sup> G. Davies, Phys. Rep. **176**, 83 (1989).
- <sup>11</sup> K. R. Elliot, Phys. Rev. B **25**, 1460 (1982).
- <sup>12</sup> E. W. Williams and H. B. Bebb, *Semiconductors and Semimetals* edited by R. A. Willardson and A. C. Beer (Academic, New York, 1972), Vol. 8, p. 321.
- <sup>13</sup> See, for example, C. T. Foxon, J. A. Harvey, and B. A. Joyce, J. Phys. Chem. Solids **34**, 1693 (1973).
- <sup>14</sup> See, for example, Y. Kanemitsu, Phys. Rep. **263**, 1 (1995); C. G. Granqvist and R. A. Buhrman, J. Appl. Phys. **47**, 2200 (1976).
- <sup>15</sup> M. V. Rama Krishna and R. A. Friesner, J. Chem. Phys. **95**, 8309 (1991).
- <sup>16</sup> See, for example, I. Mihalcescu, J. Vial, A. Bsiesy, F. Muller, R. Romestain, E. Martin, C. Delerue, M. Lannoo, and G. Allan, Phys. Rev. B **51**, 17 605 (1995).
- <sup>17</sup> H. Akiyama, S. Koshihara, T. Someya, K. Wada, H. Noge, Y. Nakamura, T. Inoshita, A. Shimizu, and H. Sakaki, Phys. Rev. Lett. **72**, 924 (1994).
- <sup>18</sup> J. Feldman, G. Peter, E. O. Gobel, P. Dawson, K. Moore, C. Foxon, and R. J. Elliot, Phys. Rev. Lett. **59**, 2337 (1987).
- <sup>19</sup> T. Itoh, M. Furumiya, T. Ikehara, and C. Gourdon, Solid State Commun. **73**, 271 (1990).
- <sup>20</sup> M. G. Bawendi, P. J. Carroll, W. L. Wilson, and L. E. Brus, J. Chem. Phys. **96**, 946 (1992).
- <sup>21</sup> M. Nirmal, D. J. Norris, M. Kuno, M. G. Bawendi, Al. L. Efros, and M. Rosen, Phys. Rev. Lett. **75**, 3728 (1995); Al. L. Efros, M. Rosen, M. Kuno, M. Nirmal, D. J. Norris, and M. Bawendi, Phys. Rev. B **54**, 4843 (1996).
- <sup>22</sup> A. Franceschetti and A. Zunger, Phys. Rev. Lett. **78**, 915 (1997); A. Franceschetti, L. W. Wang, H. Fu, and A. Zunger, Phys. Rev. B **58**, R13 367 (1998).
- <sup>23</sup> P. D. Calcott, K. J. Nash, L. T. Canham, M. J. Kane, and D. Brumhead, J. Phys.: Condens. Matter **5**, L91 (1993).
- <sup>24</sup> Y. Kanemitsu, S. Okamoto, M. Otobe, and S. Oda, Phys. Rev. B **55**, R7375 (1997); Y. Kanemitsu and S. Okamoto, *ibid.*, **58**, 9652 (1998).
- <sup>25</sup> *Semiconductors Physics of Group IV Elements and III-V Compounds*, edited by O. Madelung, M. Schulz, and H. Weiss, Ländolt-Börnstein, New Series, Group III, Vol. 17, Pt. A (Springer, Berlin, 1982).
- <sup>26</sup> The decrease of the nanocrystal size will lead to the decrease of the LO-phonon energy, because of the negative dispersion of LO phonons in GaAs nanocrystals. However, in this resonantly excited PL experiment, we cannot observe the clear size dependence of the LO-phonon energy of GaAs nanocrystals. This is because the LO-phonon-assisted PL is broad. In particular, with an increase of the excitation energy, the FLN spectra become broad, approaching the global PL spectra as shown in Fig. 7. In addition, the experimentally observed phonon energy of nanocrystals depends usually on environments and extrinsic effects (interface polarization, strains, and so on). For these reasons, it is considered that the size dependence of the LO-phonon energy is not clearly observed in GaAs/SiO<sub>2</sub> systems.
- <sup>27</sup> A. Franceschetti and A. Zunger, Appl. Phys. Lett. **68**, 3455 (1997).
- <sup>28</sup> T. Kawazoe and Y. Masumoto, Phys. Rev. Lett. **77**, 4942 (1996).
- <sup>29</sup> Y. Kanemitsu, M. Ando, H. Tanaka and T. Kushida (unpublished). Free or bound excitons nonradiatively decay through ionization, tunneling, and capture by traps at the interface and/or in the SiO<sub>2</sub> glass. After thermal annealing at high temperature 100 K, the trapped carriers release from traps and the neutralization of nanocrystals occurs. The hole-burning and hole-filling phenomena are caused by the ionization and neutralization of nanocrystals.
- <sup>30</sup> See, example, Y. Masumoto, J. Lumin. **70**, 386 (1996).
- <sup>31</sup> D. Kovalev, H. Heckler, B. Averboukh, M. Ben-Chorin, M. Schwartzkopff, and F. Koch, Phys. Rev. B **57**, 3741 (1998).
- <sup>32</sup> T. Itoh, M. Nakashima, A. I. Ekimov, C. Gourdon, Al. L. Efros, and M. Rosen, Phys. Rev. Lett. **74**, 1645 (1995).
- <sup>33</sup> K. Inoue, A. Yamanaka, K. Toda, A. V. Barabov, A. A. Onushchenko, and A. V. Fedorov, Phys. Rev. B **54**, R8321 (1996).
- <sup>34</sup> D. J. Norris, Al. Efros, M. Rosen, and M. G. Bawendi, Phys. Rev. B **53**, 16 347 (1996).
- <sup>35</sup> M. Chamarro, G. Gourdon, P. Lavallard, O. Lublinskaya, and A. I. Ekimov, Phys. Rev. B **53**, 1336 (1996).
- <sup>36</sup> J. J. Shiang, S. H. Risbud, and A. P. Alivisatos, J. Chem. Phys. **98**, 8432 (1993).
- <sup>37</sup> G. Scamarcio, V. Spagnolo, G. Ventruti, M. Lugara, and G. C. Righini, Phys. Rev. B **53**, R10 489 (1996).
- <sup>38</sup> S. Nomura and T. Kobayashi, Phys. Rev. B **45**, 1305 (1992).
- <sup>39</sup> See, for example, U. Woggon, *Optical Properties of Semiconductor Quantum Dots* (Springer, Berlin, 1997), p. 115.
- <sup>40</sup> If the interdot coupling is important in optical responses, we might observe complicated spectra due to the formation of bonding and antibonding states and the energy transfer between dots (nanocrystals). However, in the FLN and LHB experiments, there is no energy difference between the excitation laser energy and the zero-phonon-line emission. There is a good correlation between the FLN and LHB spectra of delocalized excitons.



Therefore, at present, we believe that the interdot coupling does not play an important role in the FLN and LHB spectra in our GaAs nanocrystal samples.

- <sup>41</sup>L. W. Thewalt, E. C. Lightowers, and J. I. Pankove, *Appl. Phys. Lett.* **46**, 689 (1985).
- <sup>42</sup>J. Weber, S. J. Pearton, and W. C. Dautremont-Smith, *Appl. Phys. Lett.* **49**, 1181 (1986).
- <sup>43</sup>J. Chevallier, B. Clerjaud, and B. Pajot, *Semicond. Semimet.* **34**, 447 (1991).
- <sup>44</sup>Y. Kanemitsu, H. Tanaka, K. Kushida, K. S. Min, and H. A. Atwater, *J. Lumin.* **87–89**, 432 (2000).
- <sup>45</sup>See, for example, L. Brus, *J. Phys. Chem.* **90**, 2555 (1990).
- <sup>46</sup>O. I. Micic and A. J. Nozik, *J. Lumin.* **70**, 95 (1996); A. J. Nozik and O. I. Micic, *Mater. Res. Bull.* **23**, 24 (1998).
- <sup>47</sup>M. A. Olshavsky, A. N. Goldstein, and A. P. Alivisatos, *J. Am. Chem. Soc.* **112**, 9438 (1990).